R. Mohan[1]

M. Ortiz
Mem. ASME

C. F. Shih
Mem. ASME

Division of Engineering,
Brown University,
Providence, RI 02912

Influence of Cracking Direction on Interfacial Fracture in Bicrystals With Symmetric Tilt Boundary

Recent experiments by Wang (1990) on copper bicrystals with a [110] symmetric tilt of 38.9 degrees have shown that the mode of fracture of these bicrystals, i.e., whether fracture is of a ductile or brittle nature, depends on the direction of cracking. An analysis of this effect within the framework of continuum crystal plasticity is presented. The formulation accounts for finite deformations and finite lattice rotations, as well as for the full three-dimensional collection of slip systems in FCC crystals. Our results indicate that, whereas the level of stress ahead of the crack tip is similar for the ductile and brittle cracking directions, the sizes of the plastic regions differ significantly in the two cases.

1 Introduction

The fracture properties of grain boundaries in polycrystalline metals strongly influence the behavior of the bulk material (McLean, 1957; Hirth, 1972; Watanabe, 1988; Randle and Ralph, 1988). Bicrystals constitute a convenient model system for developing an understanding of the mechanics of crystalline interfaces, and have been extensively studied in the past (Livingston and Chalmers, 1957; Hook and Hirth, 1967; Miura and Saeki, 1978; Chuang and Margolin, 1973; Rey and Zaoui, 1980). Wang and Anderson (1991) has recently conducted experiments on Cu-bicrystals with symmetric and asymmetric tilt boundaries, and found that the mode of fracture depends upon such factors as the type of interface, the amount of impurity segregation, and the direction of cracking. The directional dependence, which is the main focus of this paper, was observed in bicrystals with a [110] symmetric tilt of 38.9 deg, the interface being a $(2\bar{2}1)$ lattice plane. This tilt boundary is commonly denoted $\Sigma 9[110]/(2\bar{2}1)$. In essence, an intergranular brittle fracture surface with cleavage tongues is observed for cracking in the $[1\bar{1}4]$ direction (Fig. 7 of Wang and Anderson (1991)). By way of contrast, transgranular ductile fracture occurs for cracking in the opposite direction (Fig. 8 of Wang and Anderson, 1991).

A theoretical explanation of this effect has been attempted by Wang and Anderson (1990) and by Rice, Suo, and Wang (1990) with the aid of a modified Rice and Thomson (1975) model. In this model, the type of fracture is predicted on the basis of an analysis of the competition between cleavage and blunting by dislocation emission, with fracture presumed to be brittle when the energy release rate associated with cleavage is less than that required for dislocation emission from the tip, and ductile otherwise. Saaedvafa and Rice (1990) have carried out small-strain continuum plasticity calculations and concluded that, whereas the deformation pattern varies depending on direction, the stress levels are ostensibly identical.

In this paper we endeavor to determine whether continuum plasticity provides any indication as to the type of fracture in Wang and Anderson's $\Sigma 9$ experiment. We adopt a geometrically rigorous formulation accounting for finite deformation and finite lattice rotations, as well as the full three-dimensional geometry of the crystals. The crack is considered to be mathematically sharp in its initial configuration. We have computed crack-tip fields for two different hardening laws proposed by Peirce, Asaro, and Needleman (1981) and by Bassani and Wu (1991). Our results are consistent with Saaedvafa and Rice's (1990) observation that the levels of stress ahead of the tip are quite insensitive to the direction of cracking. However, we find that the plastic zone sizes, as defined by the isocontours of slip activity, vary substantially between directions, with the larger zones arising in the ductile case. Thus, based on this limited evidence, there appears to be some correlation between the plastic zone sizes predicted by the continuum theory and the mode of fracture. The calculated plastic zone sizes are found to vary widely depending on the choice of hardening law, with Bassani and Wu's (1991) model giving the largest differences between the ductile and brittle directions. A detailed account of the results of the calculations is given in Section 3.

2 Theory and Solution Procedure

Consider a crystal lattice being deformed from its initial undeformed configuration $\mathcal{B}_0$ to its current configuration $\mathcal{B}_t$ at time t. The deformation gradient $\mathbf{F}$ fully describes the local deformations of the crystal. We assume that two different

[1]Presently at the Department of Mechanical Engineering, University of Pennsylvania.

Contributed by the Applied Mechanics Division of THE AMERICAN SOCIETY OF MECHANICAL ENGINEERS for publication in the JOURNAL OF APPLIED MECHANICS.

Discussion on this paper should be addressed to the Technical Editor, Prof. Leon M. Keer. The Technological Institute, Northwestern University, Evanston, IL 60208, and will be accepted until two months after final publication of the paper itself in the JOURNAL OF APPLIED MECHANICS. Manuscript received by the ASME Applied Mechanics Division, Sept. 18, 1990; final revision, Mar. 15, 1991.

deformation mechanisms contribute to $\mathbf{F}$: plastic flow of the lattice due to shearing on the slip systems, which leaves the lattice invariant, and distortion of the lattice. Following Lee (1969) and others (e.g., Teodosiu, 1970; Mandel, 1972; Hill and Rice, 1972; Havner, 1973; Asaro and Rice, 1977), this suggests a multiplicative decomposition

$$\mathbf{F} = \mathbf{F}^e\mathbf{F}^p \tag{1}$$

or $\mathbf{F}$ into an elastic and plastic parts, $\mathbf{F}^e$ and $\mathbf{F}^p$, respectively. The collection of plastically deformed local configurations, defined by $\mathbf{F}^p$, are collectively referred to as the intermediate configuration $\bar{\mathcal{B}}_t$. The plastic rate of deformation relative to the crystal lattice is given by (Rice, 1971)

$$\dot{\mathbf{F}}^p\mathbf{F}^{p-1} = \sum_\alpha \dot{\gamma}^\alpha \mathbf{s}^\alpha \otimes \mathbf{m}^\alpha \tag{2}$$

where $\dot{\gamma}^\alpha$ is the shear strain rate on slip system α and $\mathbf{s}^\alpha$ and $\mathbf{m}^\alpha$ are the slip direction and slip plane normal. The sum ranges over all active slip systems.

The slip rate on system α, $\dot{\gamma}^\alpha$, is assumed to depend on stress only through the corresponding resolved shear stress

$$\tau^\alpha = \mathbf{s}^\alpha \cdot (\mathbf{F}^{eT}\boldsymbol{\tau}\mathbf{F}^{e-T}) \cdot \mathbf{m}^\alpha \tag{3}$$

where $\boldsymbol{\tau}$ is the Kirchhoff stress on $\mathcal{B}_t$. In our calculations we have adopted the power law

$$\dot{\gamma}^\alpha = \dot{\gamma}_0 \operatorname{sgn}(\tau^\alpha)\left(\frac{|\tau^\alpha|}{g^\alpha}\right)^{1/m} \tag{4}$$

where $\dot{\gamma}_0^\alpha$ is the reference shear strain rate, g^α is the current shear flow stress on slip system α, and m is the rate sensitivity exponent. For multiple slip, the evolution of the flow stresses is taken to be governed by a hardening law of the form

$$\dot{g}^\alpha = \sum_\beta h_{\alpha\beta}|\dot{\gamma}^\beta| \tag{5}$$

for some hardening moduli $h_{\alpha\beta}$. In calculations, we consider two different forms of $h_{\alpha\beta}$. In the first, henceforth referred to as the 'PAN' model for ease of reference, the moduli are assumed to be of the form proposed by Peirce, Asaro, and Needleman (1983)

$$h_{\alpha\beta} = h(\gamma)\,(q + (1-q)\delta^{\alpha\beta}) \tag{6}$$

where $\gamma = \Sigma_\alpha \gamma_\alpha$ is the sum of the accumulated slip strains on all slip systems and q characterizes the hardening behavior. The value $q = 1$, which corresponds to isotropic or Taylor hardening, has been used in our calculations. Based on the experiments of Chang and Asaro (1981), Peirce, Asaro, and Needleman (1983) proposed the expression

$$h(\gamma) = h_0 \operatorname{sech}^2\left(\frac{h_0\gamma}{\tau_s - \tau_0}\right) \tag{7}$$

as appropriate to Al-Cu alloy crystals. Here, h_0 is the initial hardening rate, τ_0 is the critical resolved shear stress, and τ_s is the saturation strength.

Based on carefully controlled latent hardening experiments in Cu single crystals (Wu, Bassani, and Laird, 1991), Bassani and Wu (1991) have recently proposed a model of hardening in single crystals, henceforth referred to as the 'BW' model, in which the hardening moduli are taken to be of the form

$$h_{\alpha\alpha} = \left[(h_0 - h_s)\operatorname{sech}^2\left(\frac{(h_0 - h_s)\gamma_\alpha}{\tau_I - \tau_0}\right) + h_s\right] \times \left(1 + \sum_{\substack{\beta \\ \beta \neq \alpha}} f_{\alpha\beta}\tanh\left(\frac{\gamma_\beta}{\gamma_0}\right)\right) \tag{8}$$

$$h_{\alpha\beta} = \epsilon h_{\alpha\alpha}$$

where τ_I is the stage I stress, i.e., the breakthrough stress where large plastic flow initiates, h_0 and h_s define the hardening slope just after initial yield and during easy glide, respectively, and ϵ is a small parameter which defines the off-diagonal terms. The functions $f\alpha\beta$ are the amplitude factors which depend on the type of dislocation junction formed between α and β slip systems. They are classified into five groups and are represented by five constants. The paper by Bassani and Wu (1991) may be consulted for details on these amplitude factors. In our calculations, we have taken $\epsilon = 0$ which corresponds to a diagonal form of the hardening moduli.

For metals, the elastic relations may be assumed to be of the simple form

$$\bar{\mathbf{S}} = \bar{\mathfrak{L}}^e\bar{\mathbf{E}}^e, \quad \bar{\mathbf{E}}^e = (\mathbf{C}^e - \mathbf{I})/2, \quad \mathbf{C}^e = \mathbf{F}^{eT}\mathbf{F}^e \tag{9}$$

without much loss of generality. Here, $\bar{\mathbf{S}} = \bar{\mathbf{F}}^{e-1}\boldsymbol{\tau}\mathbf{F}^{e-T}$ is a second Piola-Kirchhoff stress tensor relative to $\bar{\mathcal{B}}_t$, and $\bar{\mathbf{E}}^e$ and $\bar{\mathbf{C}}^e$ are the Green strain tensor and the right Cauchy-Green deformation tensor on $\bar{\mathcal{B}}_t$, respectively. To a first approximation, the elastic moduli $\mathfrak{L}^e$ for the crystals under study may be taken to be isotropic, i.e., of the form

$$\mathfrak{L}^e_{ijkl} = \lambda\delta_{ij}\delta_{kl} + \mu(\delta_{ik}\delta_{jl} + \delta_{il}\delta_{jk}) \tag{10}$$

where λ and μ are the elastic Lamé constants.

We adopt the method of solution advanced by Moran, Ortiz, and Shih (1990) in the context of flow theories of plasticity. Here, the method is generalized to handle several simultaneously active slip systems. The constitutive update is based on an *implicit* treatment of the elastic-plastic kinematics and the elastic response, defined by Eqs. (1)–(4) and (9), combined with an *explicit* treatment of the hardening laws (7) and (8), whereby the hardening moduli (6) and (8) is sampled at the start of the time step. This method of discretization results in the following algebraic equations defining the state update:

$$\begin{aligned}
&\mathbf{F}_{n+1} = \mathbf{F}^e_{n+1}\mathbf{F}^p_{n+1}, \quad \mathbf{C}^e_{n+1} = \mathbf{F}^{eT}_{n+1}\mathbf{F}^e_{n+1} \\
&(\mathbf{F}^p_{n+1} - \mathbf{F}^p_n)\mathbf{F}^{p-1}_n = \sum_\alpha \Delta\gamma^\alpha \mathbf{s}^\alpha \otimes \mathbf{m}^\alpha \\
&\Delta\gamma^\alpha = \Delta t\dot{\gamma}_0 \operatorname{sgn}(\tau^\alpha_{n+1})\left(\frac{|\tau^\alpha_{n+1}|}{g^\alpha_{n+1}}\right)^{1/m} \\
&\tau^\alpha_{n+1} = \mathbf{s}^\alpha \cdot (\mathbf{C}^e_{n+1}\bar{\mathbf{S}}_{n+1}) \cdot \mathbf{m}^\alpha \\
&g^\alpha_{n+1} = g^\alpha_n + \sum_\beta h(\gamma_n)\,(q + (1-q)\delta_{\alpha\beta})\,|\Delta\gamma^\beta| \\
&\bar{\mathbf{S}}_{n+1} = \mathfrak{L}^e : (\mathbf{C}^e_{n+1} - \mathbf{I})/2
\end{aligned} \tag{11}$$

where the subindeces $(\ )_n$ and $(\ )_{n+1}$ refer to the initial and updated values of the state variables, respectively, $\Delta\gamma^\alpha$ are the incremental slip strains, and Δt is the time increment. In (11), the final deformation gradients $\mathbf{F}_{n+1}$ are to be regarded as given. It is of interest to note that, since the hardening modulus h is treated explicitly, (11) can be reduced to a system of nonlinear equations for the incremental shear strains $\Delta\gamma^\alpha$ (for details, see Mohan, Ortiz, and Shih, 1990). In the present analysis, this system is solved by means of a local Newton-Raphson iteration with line searches. With the determination of $\Delta\gamma^\alpha$, the remaining state variables follow immediately from (11). Owing to the implicit treatment of the constitutive equations and the inclusion of the elastic response, the updated state is always unique even in the rate-independent limit, provided that the elastic domain is convex. The integration of the equilibrium equations is performed *explicitly*, by the forward-gradient method of the type proposed by Peirce, Shih, and Needleman (1984).

The finite element mesh is composed of 8-noded isoparametric brick elements. In order to prevent locking due to near incompressibility under conditions of fully developed plastic flow, we employ an assumed strain method developed by Moran, Ortiz, and Shih (1990). The method generalizes the mean-dilatation approach of Nagtegaal, Parks, and Rice (1974) to finite deformations, and consists of postulating a constant deformation Jacobian $\det(\mathbf{F})$ over each element, the value of

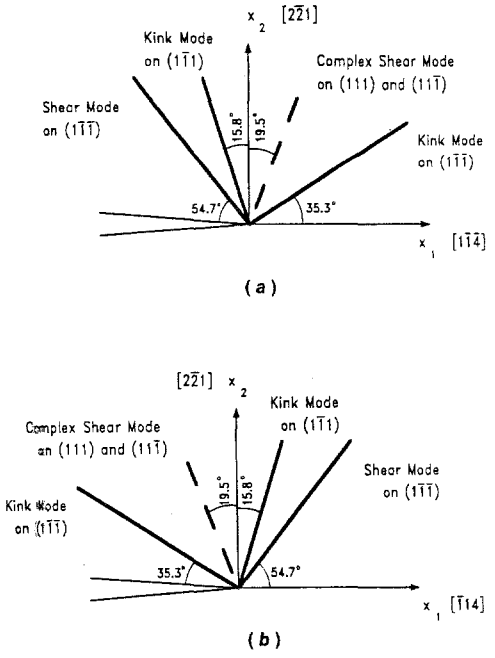

Fig. 1 The orientations of the discontinuities in the vicinity of the crack tip, based on Rice's (1987) small-strain solution, for the (*a*) [1$\bar{1}$4] (brittle) and (*b*) [$\bar{1}$14] (ductile) cracking directions

which is sampled at the centroid. The generalized plane condition is enforced by meshing a slice of the solid perpendicular to the crack front by a single layer of elements and constraining the three displacement components to be equal on both surfaces of the slice.

In the present analysis, a fan-like mesh with exponential grading in the radial direction and uniform grading in the circumferential direction is used. The ratio of the innermost to the outermost element sizes is of the order of 10^{-5}. The angular resolution of the mesh is 12 deg, and the total number of degrees-of-freedom is 5784. Tractions consistent with the linear elastic asymptotic Mode I field are distributed over the outer boundary, and increased at increments such that essentially one new ring of elements is plastified at each step. The rate of application of the loads is chosen such that the maximum strain rates in the vicinity of the crack tip are of the order of the reference strain rate $\dot{\gamma}_0$. This results in modest or negligible amounts of overstress due to rate dependency. The values of the material constants used in the calculations are: $\lambda = 576.92\tau_0$, $\mu = 384.62\tau_0$, $\dot{\gamma}_0 = 10^{-3}$, $m = 0.005$. In addition, the parameters used in describing the PAN hardening moduli are $q = 1$, $h_0 = 8.9\tau_0$, $\tau_s = 1.89\tau_0$. These values are typical of Al-Cu alloys (Chang and Asaro, 1981). For the BW hardening moduli, the parameters chosen are (Bassani and Wu, 1991): $\gamma_0 = 10^{-3}$, $h_0 = 90\tau_0$, $h_s = 1.5\tau_0$, and $\tau_I = 1.3\tau_0$. The amplitude factors $f_{\alpha\beta}$ are determined from five parameters, i.e., $a_1 = a_2 = a_3 = 8$, $a_4 = 15$ and $a_5 = 20$, (see Table 2 of Bassani and Wu, 1991).

3 Results

For the crystal orientations considered, the small-strain theory (Saeedvafa and Rice, 1990) predicts slip activity to be restricted to the six systems. For slip systems whose effective slip direction and normal lie in-plane, plastic shearing can occur either parallel or perpendicular to the slip plane. These two modes of deformation will be termed shear and kink modes, respectively. In addition, pairs of slip systems symmetrically disposed about the plane of the analysis combine to give an in-plane complex shearing mode of deformation. In Rice's theory (Rice, 1987), a set of potentially active slip systems

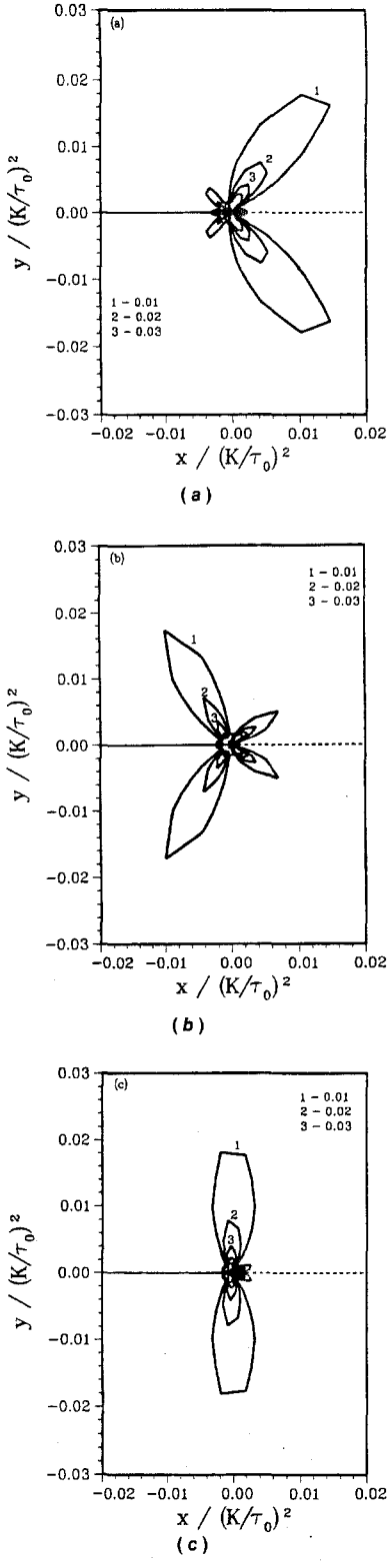

Fig. 2 Contours of slip activity, for the brittle cracking direction, on systems (*a*) (111) [101] and (111)[011], (*b*) (111) [101] and (111) [011], and (*c*) (111) [1$\bar{1}$0] and (11$\bar{1}$) [1$\bar{1}$0]. The results correspond to PAN hardening law.

involves the (1$\bar{1}\bar{1}$) or (1$\bar{1}$1) planes and effective slip in the [1$\bar{1}$2] or [$\bar{1}$12] directions due to equal and simultaneous slip along [101] and [0$\bar{1}$1] or [$\bar{1}$01], and [011], respectively. Another type of slip system involves the [1$\bar{1}$0] direction and the (111) and (11$\bar{1}$) planes. Within the framework of Rice's analysis, stress and shear displacement discontinuities arise in the vicinity of

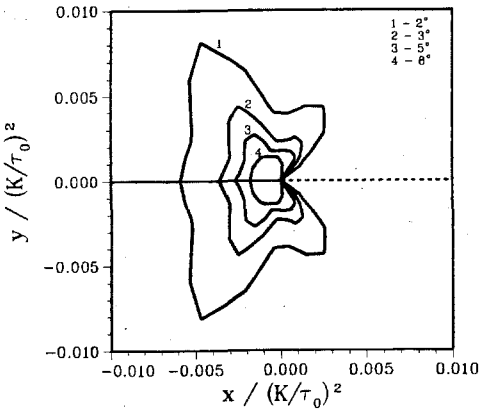

Fig. 3 Contours of lattice rotation for the brittle cracking direction predicted by PAN hardening law

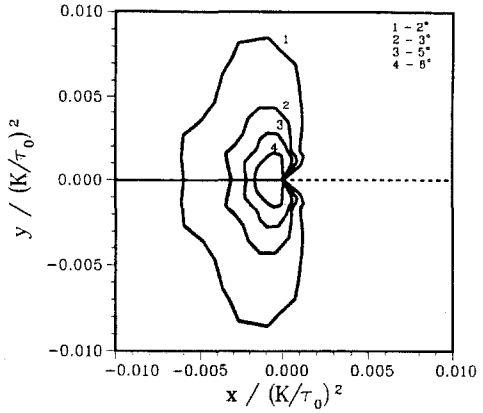

Fig. 5 Contours of lattice rotation for the ductile cracking direction predicted by PAN hardening law

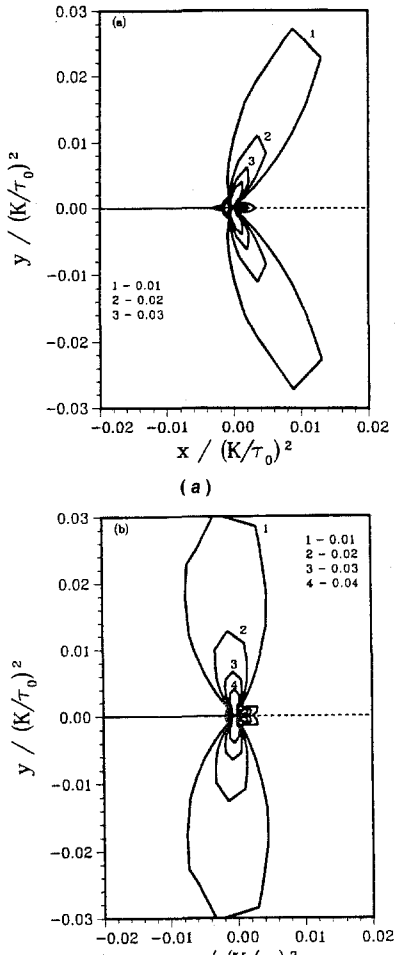

Fig. 4 Contours of slip activity, for the ductile cracking direction, on systems (*a*) (1$\bar{1}$1) [101] and (1$\bar{1}$1)[01$\bar{1}$], and (*b*) (11$\bar{1}$) [101] and (11$\bar{1}$) [011]. The results correspond to PAN hardening law.

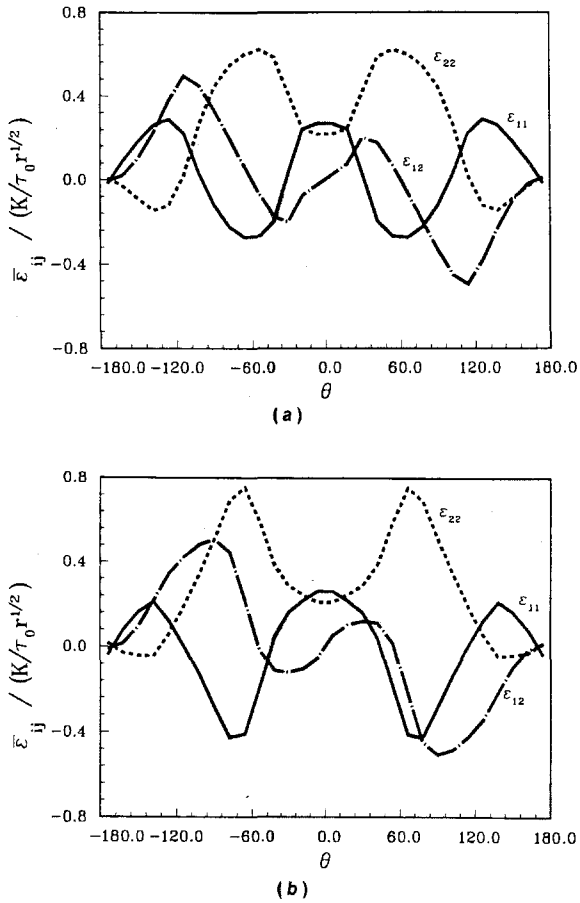

Fig. 6 Angular variation of the Almansi strain components normalized by $(K/\tau_0)r^{-1/2}$ for the (*a*) brittle, and (*b*) ductile cracking directions. The results correspond to PAN hardening law.

the crack tip which are either parallel to the active slip plane, in the shear modes, or perpendicular to it, in the kink modes. These lines of discontinuity separate sectors of constant stress.

For the specific geometry under consideration, the various sectors which define Rice's solution in the brittle and ductile cases are the reflection of each other about the [2$\bar{2}$1] direction. A shear mode and a kink mode are predicted to arise from the (1$\bar{1}\bar{1}$)-type systems. In addition, the (1$\bar{1}$1)-type systems contribute a kink mode. Complex shear involving the [$\bar{1}$10] direction and the (111) and (11$\bar{1}$) planes introduces an additional shear mode. The orientations of the resulting discontinuities are shown in Figs. 1 (*a*) and (*b*), for the ductile and brittle crack directions, respectively.

3.1 PAN Hardening Law. Contours of slip activity for the dominant slip systems when the crack is oriented along [1$\bar{1}$4] (brittle) direction are shown in Figs. 2(*a*)–(*c*). The equal and simultaneous slip activity on the (1$\bar{1}$1) [101] and (1$\bar{1}\bar{1}$)[0$\bar{1}$1]

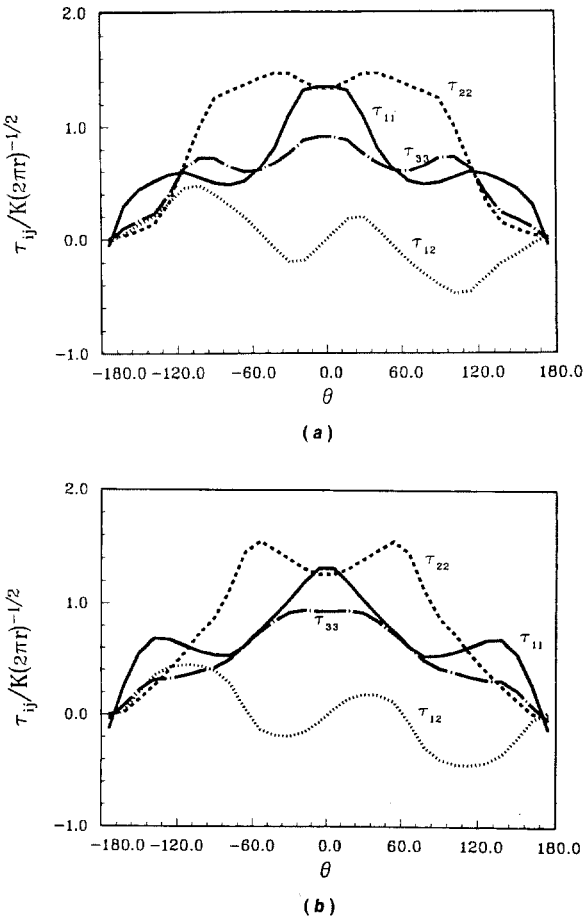

Fig. 7 Angular variation of the Kirchhoff stress components normalized by $K/\sqrt{2\pi r}$ for the (*a*) brittle and (*b*) ductile cracking directions. The results correspond to PAN hardening law.

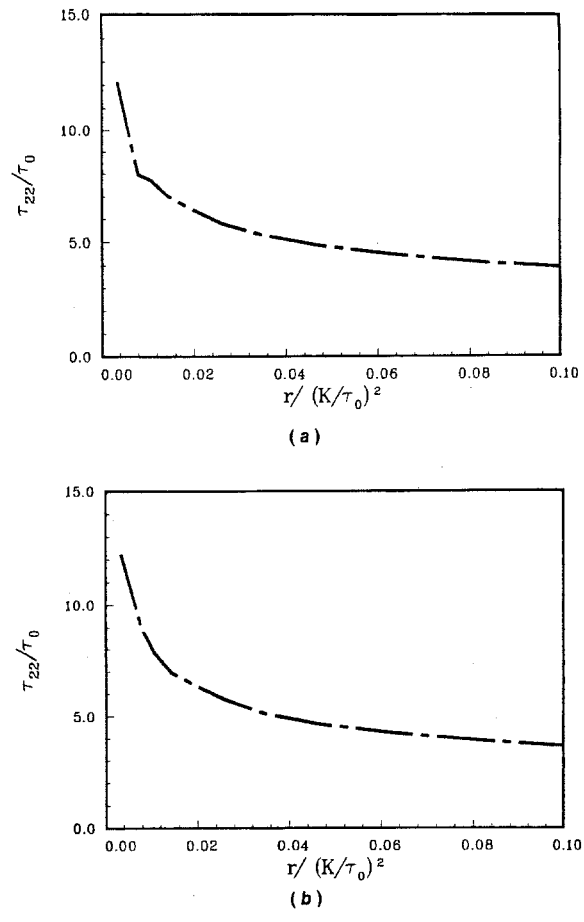

Fig. 8 Radial variation (θ = 6 deg) of the opening stress component, τ_{22}, normalized by $K/\sqrt{2\pi r}$ for the (*a*) brittle, and (*b*) ductile cracking directions. The results correspond to PAN hardening law.

systems, Fig. 2(*a*), reveals a strong kink mode at 54 deg and a weak shear mode at 144 deg. Here and subsequently, the angles subtended by the various modes are measured from the line of the crack and are determined from the corresponding maxima in the angular variations of slip strain. Slip activity on the $(1\bar{1}1)$ $[\bar{1}01]$ and $(1\bar{1}1)$ [011] systems reveals a strong kink mode at 120 deg and a relatively weak shear mode at 30 deg, Fig. 2(*b*). Figure 2(*c*) shows the contours of slip strain on the (111) $[1\bar{1}0]$ and $(11\bar{1})$ $[1\bar{1}0]$ systems. A complex shear mode at 90 deg is evident from the figure.

Some differences between the results of our calculations and Rice's (1987) asymptotic small-strain solution are noteworthy. For instance, the computed shear mode about the $(1\bar{1}1)$ plane is absent in the asymptotic solution. The reverse situation is found as regards the shear mode on $(1\bar{1}\bar{1})$: While this mode is almost absent in our computations, it does figure in Rice's solution. In addition to these differences, there are also discrepancies between the orientations of the modes which do appear in both solutions. Some of these discrepancies can be partly attributed to the intervening effect of the large lattice rotations which develop near the crack tip. Contours of lattice rotation for the brittle cracking direction are shown in Fig. 3. Interestingly, the largest rotations are observed to arise along directions which are nearly aligned with the kink modes in the solution.

For the ductile cracking direction, it is found that the complex shearing mode on slip systems (111) $[\bar{1}10]$ and $(11\bar{1})$ $[\bar{1}10]$ is nearly absent. By contrast, the contours of slip activity on the $(1\bar{1}\bar{1})$ [101] $(1\bar{1}\bar{1})$ $[0\bar{1}1]$ systems reveal a strong shear mode at 60 deg, Fig. 4(*a*). A kink mode predicted by Rice's asymptotic solution is not observed in our calculations. The slip activity on the $(1\bar{1}1)$ $[\bar{1}01]$ and $(1\bar{1}1)$ [011] systems reveals a kink mode at 90 deg, Fig. 4(*b*). Contours of the lattice rotation are shown in Fig. 5. As before, rotations are largest at 90 deg, i.e., in the direction of the kink mode. A significant difference between the two cracking directions is that the isocontours of slip activity associated with each of the operative slip systems are up to 50 percent larger in the ductile than in the brittle direction.

The angular variation of the Almansi strain components normalized by $(K/\tau_0)r^{-1/2}$ is shown in Figs. 6(*a*) and (*b*), corresponding to the brittle and ductile cracking directions, respectively. For the ductile direction, ϵ_{22} reaches a sharp peak at about 60 deg. This peak is somewhat smeared for the brittle direction. This difference is mainly due to more extensive shearing on $(1\bar{1}\bar{1})$ [101] and $(1\bar{1}\bar{1})$ $[0\bar{1}1]$ in the ductile case. The in-plane shear component ϵ_{12} has well defined peaks at 30 deg and 120 deg for the brittle cracking direction, whereas a smoother variation of this component is observed for the ductile cracking direction. Differences in slip activity of the $(1\bar{1}1)$ $[10\bar{1}]$ system account for these features.

The angular variation of the Kirchhoff stress components is shown in Figs. 7(*a*) and (*b*) for the brittle and ductile cracking directions. Of special interest is the variation of the opening stress component τ_{22} along the interface, since a high level of stress therein facilitates crack growth by cleavage. In Figs. 8(*a*) and (*b*), τ_{22} is plotted versus the distance to the crack tip at θ = 6 deg, for the ductile and brittle cracking directions. In-

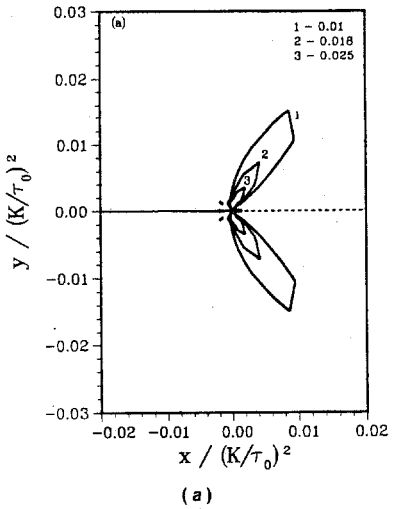

(a)

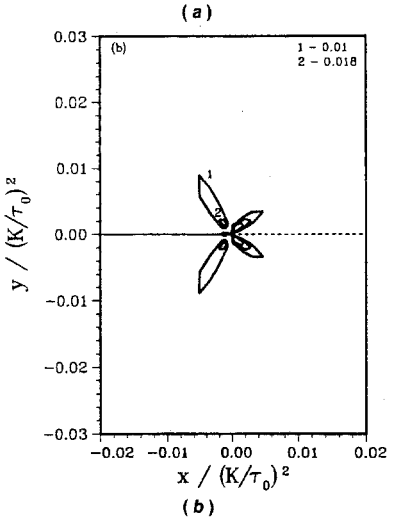

(b)

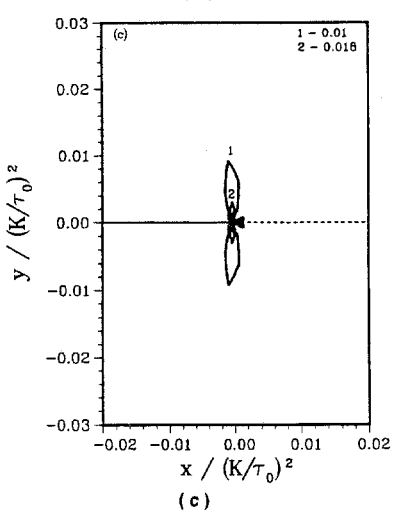

(c)

Fig. 9 Contours of slip activity, for the brittle cracking direction, on systems (*a*) (1$\bar{1}$1) [101] and (11$\bar{1}$)[01$\bar{1}$], (*b*) (111) [$\bar{1}$01] and (111) [01$\bar{1}$], and (*c*) (111) [1$\bar{1}$0] and (111) [$\bar{1}$10]. The results correspond to BW hardening law.

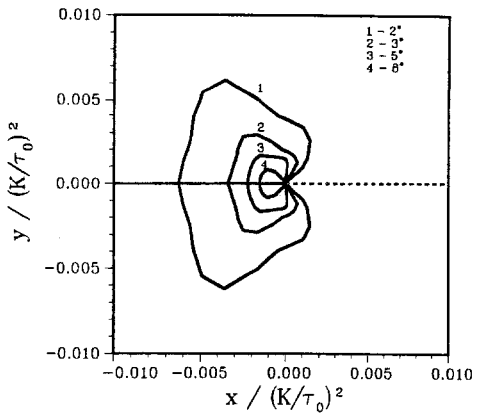

Fig. 10 Contours of lattice rotation for the brittle cracking direction predicted by BW hardening law

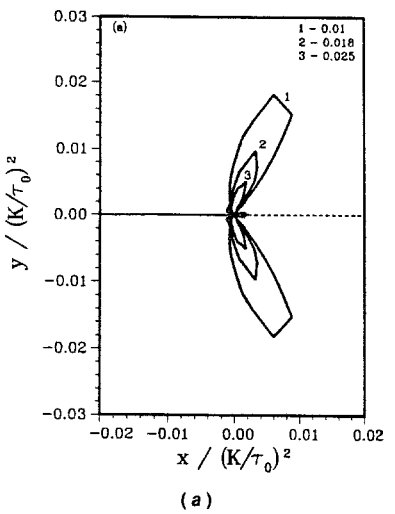

(a)

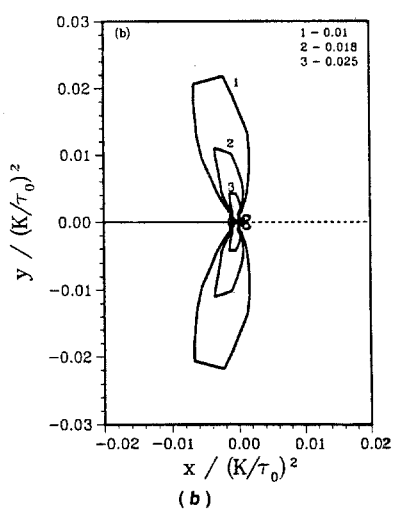

(b)

Fig. 11 Cointours of slip activity, for the ductile cracking direction, on systems (*a*) (1$\bar{1}$1) [101] and (11$\bar{1}$)[01$\bar{1}$] and (*b*) (1$\bar{1}$1) [$\bar{1}$01] and (111) [011]. The results correspond to BW hardening law.

terestingly, the levels of stress attained are quite similar in both cases. A factor contributing to this similarity may be the presence of a substantial elastic sector ahead of the tip in both cracking directions.

3.2 BW Hardening Law. Contours of slip activity on the (1$\bar{1}$1) [101] and (11$\bar{1}$) [01$\bar{1}$] systems for the cracking direction parallel to [11$\bar{4}$], i.e., for the brittle case, are shown in Fig. 9(*a*). In contrast to the predictions of the PAN hardening law, only a kink mode at 54 deg is observed in this case. The slip systems (1$\bar{1}$1) [10$\bar{1}$] and (1$\bar{1}$1) [011] give rise to both kink and shear modes, Fig. 9(*b*), of which the former is the more intense one. The slip strain contours for systems (111) [1$\bar{1}$0] and (11$\bar{1}$) [1$\bar{1}$0] reveal a complex mode at 90 deg, Fig. 9(*c*). Contours of lattice rotation for the brittle cracking direction

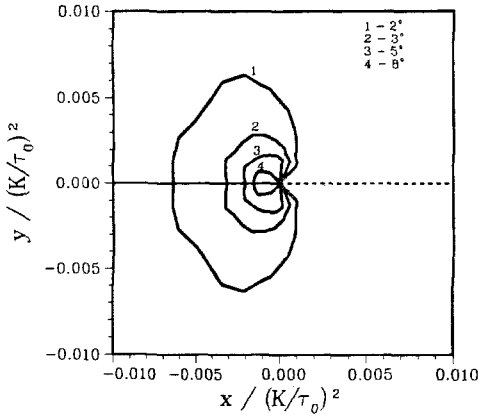

Fig. 12 Contours of lattice rotation for the ductile cracking direction predicted by BW hardening law

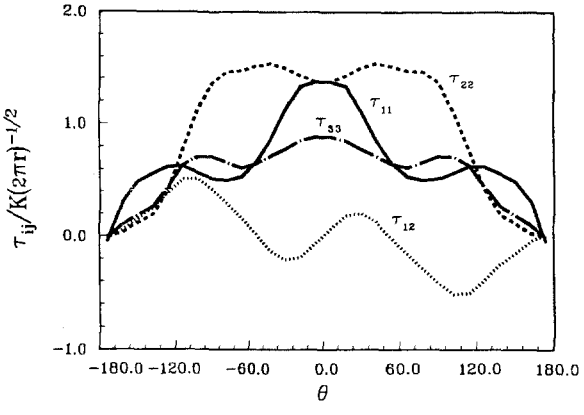

(a)

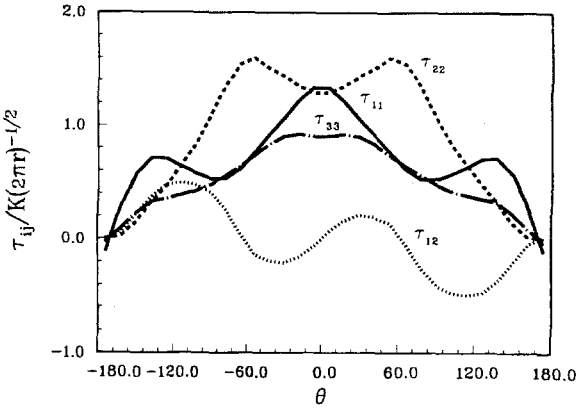

(b)

Fig. 13 Angular variation of the Kirchhoff stress components normalized by $K/\sqrt{2\pi r}$ for the (a) brittle and (b) ductile cracking directions. The results correspond to BW hardening law.

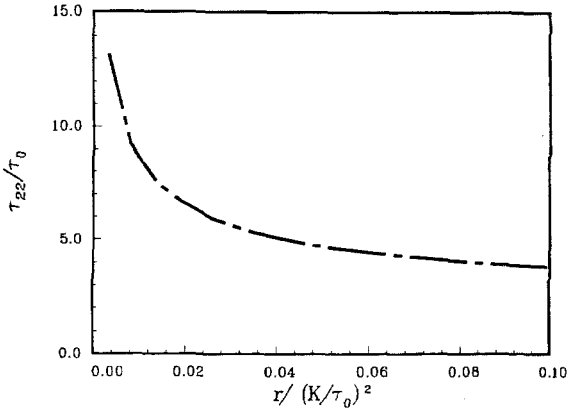

(a)

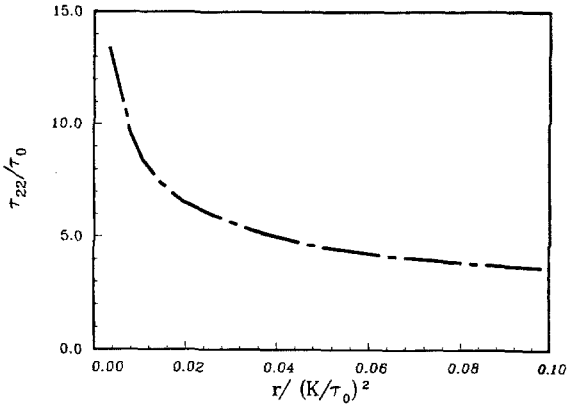

(b)

Fig. 14 Radial variation (θ = 6 deg) of the opening stress component, τ_{22}, normalized by $K/\sqrt{2\pi r}$ for the (a) brittle and (b) ductile cracking directions. The results correspond to BW hardening law.

are shown in Fig. 10. As in all the preceding cases, rotations tend to be focused in the direction of the kink mode.

For the ductile cracking direction, the complex shearing mode on slip systems (111) [$\bar{1}$10] and (1$\bar{1}$1) [$\bar{1}$10] is nearly absent. The contours of slip activity on (1$\bar{1}$1) [101] and (1$\bar{1}$1) [0$\bar{1}$1] are indicative of a strong shear mode at 60 deg, Fig. 11(*a*). In addition, a kink mode is afforded by slip systems (1$\bar{1}$1) [10$\bar{1}$] and (1$\bar{1}$1) [011], Fig. 11(*b*). The influence of the kink mode on lattice rotations is also evident in this case, Fig. 12. It is quite remarkable that the sizes of the isocontours of slip activity predicted by the BW model in the ductile case are up to twice the size of the corresponding regions in the brittle case. It therefore follows that the BW model differentiates between the ductile and brittle directions more sharply than the PAN model.

The angular variation of Kirchhoff stress components are shown in Figs. 13(*a*) and (*b*) for the brittle and ductile cracking directions. The variations are much the same as those computed from the PAN model. Likewise, the radial dependence of τ_{22} in the ductile and brittle directions, Figs. 14(*a*) and (*b*), is in close correspondence with that predicted by the PAN model. In particular, it is seen that nearly identical levels of stress are attained ahead of the tip for both the brittle and ductile directions.

4 Conclusions

We have carried out numerical simulations of recent experiments by Wang and Anderson (1991) on copper bicrystals with a [110] symmetric tilt of 38.9 deg within the framework of continuum crystal plasticity. Wang and Anderson's (1991) observations suggest that the mode of fracture of these bicrystals, i.e., whether fracture is of a ductile or brittle nature, depends on the direction of cracking. Our results show that the levels of stress which are attained ahead of the crack tip are quite insensitive to the direction of cracking, in agreement with the small-strain calculations of Saaedvafa and Rice (1990). By contrast, the plastic activity patterns are considerably more discriminating. Depending on the model of hardening adopted in the calculation the sizes of the isocontours of slip activity

for the ductile direction can be up to 50 percent (PAN model) or 100 percent (BW model) larger than those for the brittle direction. This increase in plastic activity may partially account for the transgranular and ductile character of crack growth for cracks pointing in the [$\bar{1}$14] direction.

There is not enough experimental evidence at this point to permit a clear assessment of the role of continuum plasticity effects in determining the ductile versus brittle character of cracking along bicrystal interfaces. However, our results seem to suggest that some correlation may exist between plastic zone size and fracture mode. The fact that plastic zone size predictions are so sensitive to the hardening model points to the need to develop physically based and accurate hardening laws before calculations can be made more predictive.

Acknowledgments

The support of the National Science Foundation through the Materials Research Group at Brown University, Grant DMR-9002994, is gratefully acknowledged. We are also indebted to J. R. Rice and M. Saeedvafa for making available to us the results of their computations.

References

Asaro, R. J., 1983, "Micromechanics of Crystals and Polycrystals," *Advances in Applied Mechanics*, Vol. 23, pp. 1–115.

Asaro, R. J., and Rice, J. R., 1977, "Strain Localization in Ductile Single Crystals," *Journal of the Mechanics and Physics of Solids*, Vol. 25, pp. 309–338.

Bassani, J. L., and Wu, T.-Y., 1991, "Latent Hardening in Single Crystals: Part 2, Analytical Characterization and Predictions," *Proceedings of Royal Society of London*, Vol. A435, pp. 21–41.

Bilby, B. A., Cottrell, A. H., and Swinden, K. H., 1963, "The Spread of Plastic Yield from a Notch," *Proceedings of the Royal Society, London*, Vol. A272, pp. 304–314.

Chang, Y. W., and Asaro, R. J., 1981, "An Experimental Study of Shear Localization in Aluminum-Copper Single Crystals," *Acta Metallurgica*, Vol. 29, pp. 241–257.

Chaung, Y.-D., and Margolin, H., 1973, "Brass Bicrystal Stress-Strain Relations," *Metallurgical Transactions*, Vol. 4, pp. 1905–1917.

Havner, K. S., 1973, "On the Mechanics of Crystalline Solids," *Journal of the Mechanics and Physics of Solids*, Vol. 21, pp. 383–394.

Hill, R., and Rice, J. R., 1972, "Constitutive Analysis of Elastic-Plastic Crystals at Arbitrary Strain," *Journal of the Mechanics and Physics of Solids*, Vol. 20, pp. 401–413.

Hirth, J. P., 1972, "The Influence of Grain Boundaries on Mechanical Properties," *Metallurgical Transactions*, Vol. 3, pp. 3047–3067.

Hook, R. E., and Hirth, J. P., 1967, "The Deformation Behaviour of Isoaxial Bicrystals of Fe-3% Si," *Acta Metallurgica*, Vol. 15, pp. 535–551.

Kelly, A., Tyson, W. R., and Cottrell, A. H., 1967, "Ductile and Brittle Crystals," *Philosophical Magazine*, Vol. 15, pp. 567–586.

Lee, E. H., "Elastic-Plastic Deformation at Finite Strains," ASME JOURNAL OF APPLIED MECHANICS, Vol. 36, pp. 1–6.

Livingston, J. D., and Chalmers, B., 1957, "Multiple Slip in Bicrystal Deformation," *Acta Metallurgica*, Vol. 5, pp. 322–327.

McLean, D., 1957, *Grain Boundaries in Metals*, Oxford University Press, Oxford, U.K.

Mandel, J., 1972, *Plasticité Classique et Viscoplasticité*, Course given at Int. Centre for Mech. Sci., Udine 1971, Springer, Berlin.

Miura, S., and Saeki, Y., 1978, "Plastic Deformation of Aluminum Bicrystals ⟨100⟩ Oriented," *Acta Metallurgica*, Vol. 26, pp. 93–101.

Mohan, R., Ortiz, M., and Shih, C. F., 1990, "An Analysis of Cracks in Ductile Single Crystals: Part I—Anti-Plane Shear," *Journal of Mechanics and Physics of Solids*, to appear.

Moran, B., Ortiz, M., and Shih, C. F., 1990, "Formulation of Implicit Finite Element Methods for Multiplicative Finite Deformation Plasticity," *International Journal for Numerical Methods in Engineering*, Vol. 29, pp. 483–514.

Nagtegaal, J. D., Parks, D. M., and Rice, J. R., 1974, "On Numerically Accurate Finite Element Solutions in the Fully Plastic Range," *Computer Methods in Applied Mechanics and Engineering*, Vol. 4, pp. 153–177.

Peirce, D., Asaro, R. J., and Needleman, A., 1983, "Material Rate Dependence and Localized Deformation in Crystalline Solids," *Acta Metallurgica*, Vol. 31, pp. 1951–1976.

Peirce, D., Shih, C. F., and Needleman, A., 1984, "A Tangent Modulus Method for Rate Independent Solids," *Computers and Structures*, Vol. 18, pp. 875–887.

Randle, V., and Ralph, B., 1988, "Applications of Grain Boundary Engineering to Anamolous Grain Growth," *Interfacial Structure, Properties and Design*, Vol. 122, M. H. Yoo et al., eds., MRS, Pittsburgh, pp. 419–424.

Rey, C., and Zaoui, A., 1980, "Slip Heterogeneities in Deformed Aluminum Bicrystals," *Acta Metallurgica*, Vol. 28, pp. 687–697.

Rice, J. R., 1971, "Inelastic Constitutive Relations for Solids: An Internal-Variable Theory and Its Application to Metal Plasticity," *Journal of the Mechanics and Physics of Solids*, Vol. 19, pp. 443–455.

Rice, J. R., 1987, "Tensile Crack Tip Fields in Elastic-Ideally Plastic Crystals," *Mechanics of Materials*, Vol. 6, pp. 317–335.

Rice, J. R., Suo, Z., and Wang, J.-S., 1990, "Mechanics and Thermodynamics of Brittle Interfacial Failure in Bimaterial Systems," *Proceedings of Acta/Scripta Metallurgical Conference on Bonding, Structure and Mechanical Properties of Metal/Ceramic Interfaces*, M. Ruhle et al., eds., Pergamon Press, New York, pp. 269–294.

Rice, J. R., and Thomson, R., 1974, "Ductile Versus Brittle Behaviour of Crystals," *Philosophical Magazine*, Vol. 29, pp. 73–97.

Saeedvafa, M., and Rice, J. R., 1990, work in progress, Harvard University.

Teodosiu, C., 1970, "A Dynamic Theory of Dislocations and its Applications to the Theory of Elastic-Plastic Continuum," *Fundamental Aspects of Dislocation Theory*, Vol. II, J. A. Simmons et al., eds., U.S. National Bureau of Standards U.S. Special Publication, pp. 837–876.

Wang, J.-S., and Anderson, P., 1991, "Fracture Behaviour of Embrittled F.C.C. Metal Bicrystals," *Acta Metallurgica*, Vol. 39, pp. 779–792.

Watanabe, T., 1988, "The Importance of Grain Boundary Character Distribution to Grain Boundary Design," *Interfacial Structure, Properties and Design*, Vol. 122, M. H. Yoo et al., eds., MRS, Pittsburgh, pp. 443–454.

Wu, T.-Y., Bassani, J. L., and Laird, C., 1991, "Latent Hardening in Single Crystals: Part 1, Experimental Characterization," *Proceedings of Royal Society of London*, Vol. A435, pp. 1–19.